Sains Malaysiana 55(5)(2026): 867-877
http://doi.org/10.17576/jsm-2026-5505-09

Geothermal Resource Potential in Zamfara Area, North-Western Nigeria: Insights from Airborne Magnetic Data

(Potensi Sumber Geoterma di Kawasan Zamfara, Barat Laut Nigeria: Pemerhatian daripada Data Magnetik Udara)

SABIU BALA MUHAMMAD[1,2], NORDIANA MOHD MUZTAZA[1,*], UMAYYA SIYAMA MUSA[2], NUR AZWIN ISMAIL[1], SYA'RAWI MUHAMMAD HUSNI MOHD SHARONI[1], MUHAMMAD TAQIUDDIN ZAKARIA[3], BABANGIDA MOHAMMED AHMED[1,4], MUSTAPHA ADEJO MOHAMMED[5] & SIRAJO ABUBAKAR[6]

[1]*School of Physics, Universiti Sains Malaysia, 11800 Penang, Malaysia*
[2]*Department of Physics, Usmanu Danfodiyo University, P.M.B. 2346 Sokoto, Nigeria*
[3]*Department of Earth Sciences and Environment, Faculty of Science and Technology, Universiti Kebangsaan Malaysia, 43600 UKM Bangi, Selangor, Malaysia*
[4]*Department of Applied Physics, Federal University of Technology Babura, Jigawa State, Nigeria*
[5]*Department of Physics, Federal University Lafia, Nasarawa State, Nigeria*
[6]*Department of Physics, Sokoto State University, Sokoto, Nigeria*

Received: 22 December 2025/Accepted: 30 April 2026

ABSTRACT

The transition to sustainable energy in Nigeria requires a precise characterization of untapped geothermal reservoirs; however, the thermal architecture of the northern basement complexes remains largely unexplored. To address this, the geothermal resource potential of the Zamfara State sector within the Northern Nigerian Basement Complex was evaluated using airborne magnetic data. This evaluation provides the empirical framework necessary to guide future energy exploration and development in the region. The area covers approximately 12,100 km² between longitudes 5°30′E-6°30′E and latitudes 12°00′N-13°00′N. The magnetic data showed significant variations in total magnetic intensity, with high anomalies corresponding to granitic intrusions, migmatite-gneiss units and banded iron formations, while low anomalies align with the thin sedimentary cover of the Sokoto Basin. Spectral depth analysis indicated shallow magnetic sources (0.25-0.36 km) associated with near-surface intrusions and deeper sources (2.36-7.52 km) representing the Precambrian basement. Curie point depth estimates ranged from 4.39 to 14.69 km, reflecting the influence of heat-producing granitic lithologies on the crustal thermal regime. A range of values from 39.47 to 131.89 °C/km were obtained for geothermal gradients and heat flow ranged from 98.68-329.73 mWm^{-2}, with the highest values observed around the Maru and Bungudu areas. Radiogenic heat production exhibits spatial variability, reaching up to 6.51 $\mu W/m^3$ in dominant granitic regions. These results demonstrate a strong geological control on magnetic and thermal properties, highlight areas of anomalous geothermal potential and provide a robust framework for future geothermal exploration in the area.

Keywords: Geothermal energy; magnetic data; Zamfara area

ABSTRAK

Peralihan kepada tenaga lestari di Nigeria memerlukan pencirian tepat bagi takungan geotermal yang belum diterokai; namun, seni bina terma kompleks batuan dasar utara masih belum banyak diterokai. Bagi menangani perkara ini, potensi sumber geotermal di sektor negeri Zamfara dalam Kompleks Batuan Dasar Utara Nigeria telah dinilai menggunakan data magnetik udara. Penilaian ini menyediakan rangka kerja empirik yang diperlukan untuk membimbing penerokaan dan pembangunan tenaga pada masa hadapan di rantau tersebut. Kawasan kajian meliputi kira-kira 12,100 km² antara longitud 5°30′T-6°30′T dan latitud 12°00′U-13°00′U. Data magnet menunjukkan variasi ketara dalam keamatan magnet keseluruhan dengan anomali tinggi berkaitan dengan penerobosan granit, unit migmatit-gneis dan formasi besi berjalur, manakala anomali rendah sejajar dengan litupan sedimen nipis Lembangan Sokoto. Analisis kedalaman spektrum menunjukkan sumber magnet cetek (0.25-0.36 km) yang dikaitkan dengan penerobosan berhampiran permukaan serta sumber yang lebih dalam (2.36-7.52 km) yang mewakili batuan dasar kambria awal. Anggaran kedalaman titik Curie berjulat antara 4.39 hingga 14.69 km, mencerminkan pengaruh litologi granit penghasil haba terhadap rejim terma kerak. Kecerunan geoterma berbeza antara 39.47 hingga 131.89 °C/km, manakala aliran haba berada dalam julat 98.68-329.73 mWm^{-2} dengan nilai tertinggi diperhatikan di sekitar kawasan Maru dan Bungudu. Penghasilan haba radiogenik juga menunjukkan variasi ruang, mencapai sehingga 6.51 $\mu W/m^3$ di kawasan yang didominasi oleh batuan granit. Hasil kajian ini menunjukkan kawalan geologi yang kuat terhadap sifat magnet dan terma, menonjolkan kawasan berpotensi geoterma anomali, serta menyediakan kerangka yang mantap untuk penerokaan geoterma pada masa hadapan di kawasan tersebut.

Kata kunci: Data magnetik; kawasan Zamfara; tenaga geoterma

INTRODUCTION

Energy derives virtually every aspect of modern life, from basic human activities to large-scale industrial processes. As population growth and industrialization continue to accelerate, reliance on non-renewable energy resources has intensified which leads to their rapid depletion. This underscores the urgent need to identify and develop alternative, sustainable energy sources capable of meeting rising global energy demands. Of these alternatives, geothermal energy represents a promising and largely underutilized resource. Its effective development depends on detailed subsurface investigations which can be achieved through geophysical methods designed to delineate potential energy reservoirs (Shlof et al. 2025; Yusuf, Lim & Abir 2022).

Geophysical surveys involve the measurement of physical parameters of the Earth's interior to infer its composition, structure and origin (Muhammad et al. 2020a). A sound understanding of subsurface properties provides the foundation for identifying and harnessing exploitable energy resources. Several geophysical techniques are commonly applied for this purpose, each governed by a specific physical property that determines its suitability. These include electrical, seismic, radiometric, gravity and magnetic methods (Simon et al. 2026; Zakaria et al. 2024). The magnetic method, in particular, is well suited for detecting buried magnetic sources due to contrasts in magnetic susceptibility. Magnetic data may be acquired through ground, marine, or aeromagnetic surveys with applications in mineral exploration, engineering and construction investigations, archaeology, hydrocarbon exploration, and geothermal studies (Zakaria et al. 2025). Importantly, magnetic methods allow for the estimation of sediment thickness and temperature gradients. The two are the most critical parameters for determining heat flow, which is essential for evaluating geothermal potential.

High-resolution aeromagnetic surveys are effective for geothermal exploration over large areas. Such surveys can be used to identify concealed intrusive bodies, delineate basement structures and detect zones of reduced magnetization associated with elevated temperatures at depth, commonly expressed as the Curie point depth (Boumehdi et al. 2025). Estimation of the Curie isotherm, when combined with heat-flow analysis, provides valuable insight into crustal temperature distributions and helps address the persistent lack of subsurface thermal data in many regions. Variations in Curie depth have been shown to reflect regional thermal regimes and the concentration of geothermal energy at depth (Musa, Garba & Kamureyina 2025).

Geothermal energy refers to the heat generated and stored within the Earth. It represents a renewable and sustainable energy source. It has the potential to provide reliable electricity for domestic, industrial, agricultural and recreational uses. Globally, increasing emphasis has been placed on geothermal energy due to its numerous advantages. They include continuous power generation, minimal environmental impact, low greenhouse-gas emissions and widespread availability (Sui et al. 2019). In Nigeria, where energy production is dominated by hydrocarbons, electricity supply remains inadequate relative to growing demand. Rapid population growth, coupled with limited expansion in energy generation capacity, has exacerbated this imbalance. At the same time, increasing concern over environmental pollution has renewed interest in cleaner and more sustainable energy options (Nwankwo & Shehu 2015).

Geothermal energy offers a viable pathway toward addressing these challenges. It is an abundant, secure and environmentally friendly energy source derived from heat associated with sedimentary basin formations and radioactive decay within basement complex rocks (Ejike et al. 2025). However, geothermal research in Nigeria remains limited, resulting in a significant gap in knowledge of crustal temperature distribution and heat-flow characteristics. Addressing this gap is essential for informed energy planning and diversification.

The aim of this study was to evaluate the geothermal energy potential at Gandi, Talata Mafara, Anka and Maru areas of Zamfara State, Nigeria, using aeromagnetic data. Specifically, the study seeks to estimate the Curie point depth, geothermal gradient, heat-flow distribution and radiogenic heat production within the study area. The findings are expected to contribute to an improved understanding of the region's geothermal prospects and support efforts toward sustainable energy development in Nigeria.

GEOLOGICAL SETTING

The study area is located within the Northern Nigerian Basement Complex. It extends between longitudes 5°30′E and 6°30′E and latitudes 12°00′N and 13°00′N, covering an area of approximately 12,100 km² (Figure 1). Geologically, the area is dominated by Upper Proterozoic crystalline basement rocks that have undergone multiple episodes of deformation, metamorphism and magmatic intrusion, resulting in a complex assemblage of lithologies that exert strong control on the region's magnetic and geothermal characteristics (Muhammad, Ogunsina & Muztaza 2025b).

Approximately 90% of the area is underlain by crystalline basement rocks typical of north-western Nigeria (Oluyide et al. 2023). These include migmatites, gneisses, schists, granites and granodiorites belonging to the Migmatite-Gneiss Complex and the Older Granites (Figure 1). The Migmatite-Gneiss Complex ranges in age from Meso-Archean to Neo-Proterozoic (approximately 3200-542 Ma). It consists mainly of migmatites, banded gneisses and schists that are commonly foliated and locally intruded by granitoids. These rocks are characterised by variable magnetic susceptibilities, reflecting differences in mineral composition, degree of metamorphism and structural fabric (Aliyu 2024).

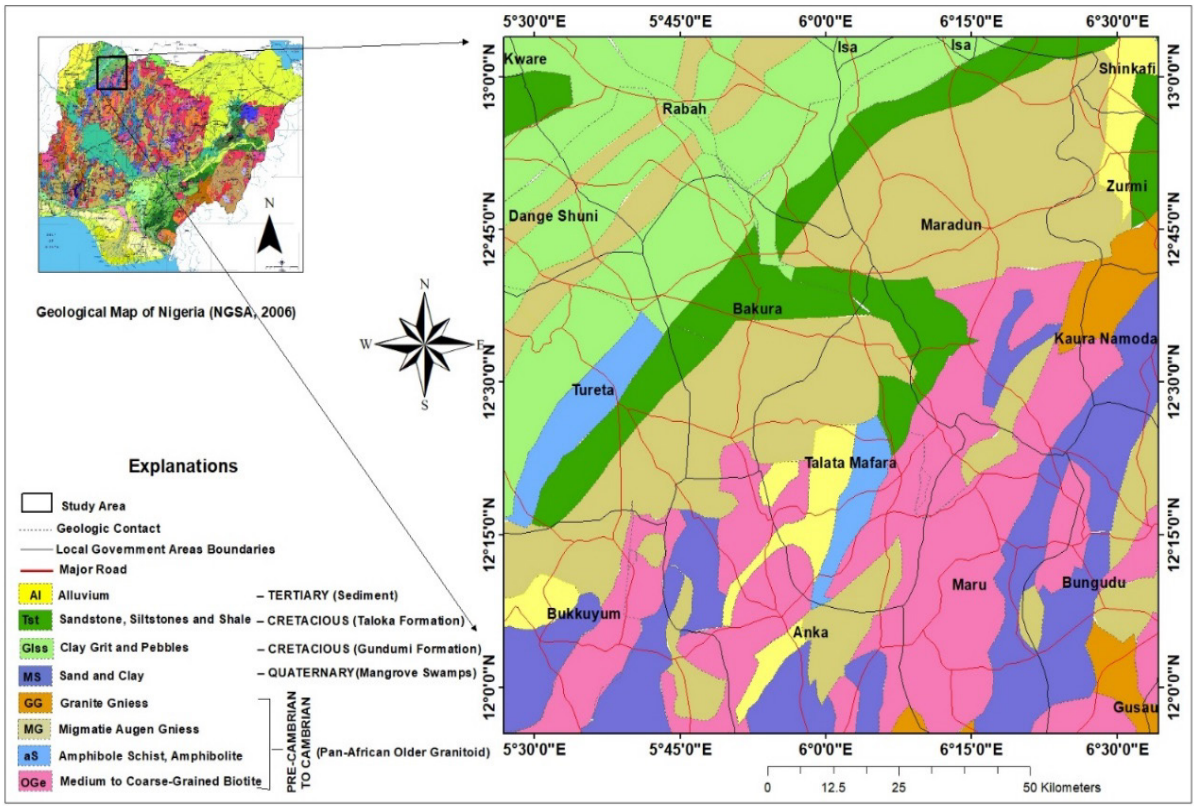

FIGURE 1. Geological map of the study area (adapted from NGSA)

Supracrustal rocks, including quartzites, phyllites, slates, and metaconglomerates, occur as infolded belts within the migmatite-gneiss complex. Pelitic units are widespread and commonly interlayered with siltstones. Of particular geophysical significance are banded iron formations composed predominantly of magnetite, hematite and garnet. These locally enhance magnetic responses and contribute to the observed magnetic highs within the basement terrain.

The Older Granites are of Pan-African age (approximately 800-400 Ma). They comprise granites, granodiorites, diorites, and dolerites that intruded the Migmatite-Gneiss Complex during the Pan-African orogenic event. These granitoids are typically enriched in radiogenic elements such as uranium, thorium, and potassium, making them important contributors to crustal heat production and elevated geothermal gradients observed in parts of the study area.

Younger Granites associated with the Mada and Afu ring complexes occur near the north-western margin of the study area. These anorogenic, high-level intrusions are Triassic to Jurassic in age (approximately 210-145 Ma). They consist mainly of microgranites and biotite granites (Turner 2025). Their emplacement is associated with crustal thinning and magmatic heat input, which may further influence the thermal structure and Curie point depth variations inferred from aeromagnetic data.

The remaining approximately 10% of the study area is occupied by sedimentary units of the Sokoto (lower Iullemmeden) Basin. It comprises mainly clays, sandstones, and pebble beds of lacustrine to fluviatile origin (Muhammad et al. 2025). These sediments rest unconformably on the crystalline basement and attain a maximum thickness of about 300 m near the Niger border. The basal part of the succession is marked by conglomeratic beds exposed at Tureta and Ruwan Kalgo, with additional exposures along the Zamfara and Dutsin Dambo rivers near Bakura (Shuaibu et al. 2022). The relatively thin sedimentary cover contributes to subdued magnetic signatures and shallow depths to magnetic sources in these areas.

Overall, the interplay between crystalline basement lithologies, granitic intrusions, structural features and limited sedimentary cover defines the geologic framework of the study area and provides a robust basis for interpreting the observed magnetic anomalies, depth-to-basement estimates, Curie point depths and geothermal characteristics.

METHODOLOGY

Four airborne magnetic maps covering sheets 30, 31, 52, and 53 – corresponding to the Gandi, Talata Mafara, Anka, and Maru areas – were analysed and interpreted in this

study. The datasets were obtained from the nationwide airborne geophysical survey conducted by Fugro and sponsored by the Nigerian Geological Survey Agency (NGSA). Data acquisition was carried out along northwest-southeast flight lines spaced at 500 m, with an average terrain clearance of 80 m and tie-line spacing of 2 km (Muhammad & Saad 2018a). The total area investigated covered approximately 12,100 km². With a line spacing of 500 m, the Nyquist frequency of our dataset is 1 cycle/km. According to the sampling theorem, features smaller than 2Δx (1 km) cannot be uniquely resolved without aliasing. Consequently, while this resolution is robust for estimating the Curie Isothermal Depth (CPD) and identifying large-scale crustal heat sources, it acts as a low-pass filter that may overlook small-scale, shallow (<1 km depth) volcanic plugs or localized hydrothermal conduits. However, spectral methods used for Curie point depth estimation in this study rely primarily on long-wavelength components of the magnetic field, which are adequately resolved by the dataset.

The four aeromagnetic sheets were assembled, gridded and merged using Oasis Montaj software to generate a composite Total Magnetic Intensity (TMI) map of the study area. To improve anomaly positioning in this low-latitude region, the TMI data were transformed using the Reduction to the Equator (RTE) filter. This correction shifted magnetic anomaly maxima closer to their causative sources, thereby enhancing structural interpretation (Muhammad et al. 2020b; Vihywuseh et al. 2025).

The observed TMI field comprised both regional and residual magnetic components. The regional component represented long-wavelength magnetic effects from deep sources, whereas the residual component reflected magnetic responses from crustal rocks. To isolate the residual anomalies relevant to crustal structure and geothermal interpretation, the regional magnetic field was modelled as a first-order polynomial surface and removed from the TMI data following the method of Dobrin (1976). The residual magnetic field was obtained by fitting and subtracting a linear trend surface using multiple regression techniques (Muhammad & Saad 2018b). This residual dataset was subsequently used for spectral and thermal analyses.

The spectral analysis was performed to estimate depths to magnetic sources and derive geothermal parameters. The residual magnetic anomaly map was subdivided into twenty-five (25) equal-sized $\frac{1^0}{2} \times \frac{1^0}{2}$ (55.5 km × 55.5 km) overlapping blocks to ensure statistical validity. To reduce spectral noise, the overlap percentage was varied at 25%, 50% and 75%. A Fast Fourier Transform (FFT) was applied to each block to convert the spatial data into the frequency domain. For each block, the logarithm of spectral energy was plotted against frequency (cycles per metre). The resulting spectra typically displayed two linear segments, corresponding to shallow and deep magnetic source ensembles.

The slopes of the high- and low-frequency segments were used to estimate the depth to the centroid (Z_0) and the depth to the top boundary (Z_t) of the magnetic sources, respectively (Figure 2) (Okubo et al. 1985). The Curie point depth (Z_b) representing the basal depth of magnetised crust, was then calculated using the relation proposed by Tanaka, Okubo and Matsubayashi (1999):

$$Z_b = 2Z_o - Z_t \quad (1)$$

Assuming a Curie temperature of 580 °C for magnetite, the geothermal gradient was estimated as the ratio of Curie temperature to Curie point depth. Heat flow was subsequently computed using Fourier's law, adopting a thermal conductivity value of 2.5 W m^{-1} $°C^{-1}$, which is considered representative of the crystalline basement rocks in the study area (Harash & Chen 2022). These parameters were directly used to assess the spatial variation of geothermal conditions discussed in the Results section.

Radiogenic heat production (RHP), arising from the decay of radioactive isotopes such as Uranium (^{238}U), Uranium (^{235}U), Thorium (^{232}Th), and Potassium (^{40}K) within the crust, was also evaluated. Depth-dependent radiogenic heat production was calculated using an exponential decay model, assuming a surface heat production of 1.5 μW m^{-3} (Jiang et al. 2025) and a radiogenic scaling depth of 10 km (Adetona et al. 2024). The estimated RHP values complemented the heat-flow results and supported the thermal interpretation presented in the Discussion section.

Finally, the derived Curie point depth, geothermal gradient, heat flow and radiogenic heat production values were imported into Surfer software to generate two-dimensional contour maps. These maps were used to analyse the spatial distribution of geothermal parameters and to establish relationships between magnetic structure and thermal regime, which are discussed in the Results and Discussion sections.

RESULTS AND DISCUSSION

The Total Magnetic Intensity (TMI) map of the study area is presented in Figure 3(a). It was generated after gridding and merging the HRAM datasets and removing a constant magnetic field value of 33,000 nT. It showed magnetic intensity values ranging from −71.7 to 145.0 nT. These variations indicated the presence of significant magnetic features, which are consistent with the lithological heterogeneity of the migmatite-gneiss complex that dominates the study area. Variations in magnetic signature were attributed to contrasts in lithology, magnetic susceptibility, depth to magnetic sources, structural discontinuities and variations in geological strike.

Areas characterised by low magnetic anomalies (blue tones) were predominantly distributed across the north-eastern part and scattered throughout the study area. They suggest lower concentrations of magnetically susceptible

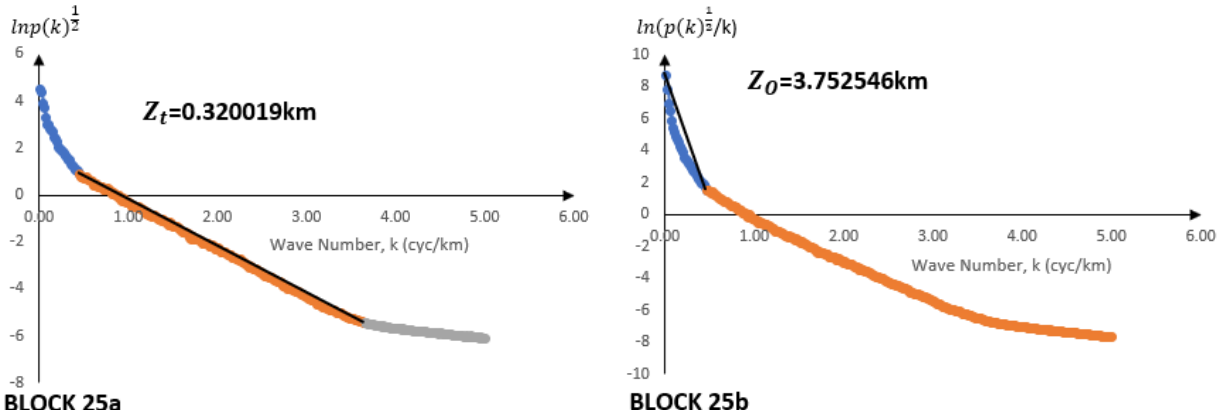

FIGURE 2. Sample plot of log of spectral energy against frequency for block 25

minerals. In contrast, regions of high magnetic anomalies (pink tones) were concentrated mainly in the southern and north-eastern parts, with fewer occurrences in the north-western region. These high-amplitude anomalies were interpreted to reflect zones enriched in magnetically susceptible minerals, likely associated with crystalline basement rocks or intrusive bodies. Localised high-amplitude magnetic anomalies may also be enhanced by the presence of banded iron formations containing magnetite and hematite, which are reported within the migmatite-gneiss complex of the study area.

To enhance anomaly positioning and improve structural interpretation, the TMI data were transformed using RTE filter (Figure 3(b)), as described in the Methodology section. This correction effectively centred the magnetic anomalies over their causative sources without significantly altering their amplitudes, thereby preserving the geophysical meaning of the data. The RTE-transformed data were subsequently subjected to first-order polynomial fitting to remove the regional magnetic field and isolate the residual component.

The regional magnetic field map (Figure 4(a)) exhibited a dominant NW-SE trend with magnetic values increasing from the south-western (blue tones) to the north-eastern (pink tones) portions of the study area. Regional field values ranged between 41.7 and 65.3 nT after removing 33,000 nT uniform field, reflecting deep-seated magnetic contributions consistent with large-scale basement structures.

Figure 4(b) shows the residual magnetic anomaly map. The figure displayed pronounced magnetic highs and lows with values ranging from −116.9 to 86.9 nT. Negative anomalies were interpreted as magnetically subdued zones. Although approximately 10% of the study area is covered by the Sokoto Basin with sediment thicknesses of up to ~300 m, this relatively thin sedimentary cover is unlikely to significantly influence the regional magnetic field. The observed low magnetic anomalies are therefore more plausibly attributed to variations in the underlying basement composition, such as low-susceptibility lithologies or altered zones, with the sedimentary cover contributing only minor attenuation of shallow magnetic responses. The positive anomalies represented magnetically responsive zones. These high-amplitude anomalies were attributed to crystalline igneous or metamorphic rocks, deep-seated volcanic bodies or major crustal boundaries, consistent with interpretations of basement terrains. The residual magnetic field formed the basis for spectral analysis.

Quantitative interpretation of the residual magnetic field was carried out using spectral depth analysis, following the FFT-based approach outlined in the Methodology section. Contour maps derived from the spectral results presented in Figure 5(a) & 5(b). They showed spatial variations in the depth to the top (Z_t) and depth to the centroid (Z_o) of magnetic sources. The shallow magnetic sources (Z_t) ranged from 0.25 to 0.29 km in the extreme north-western part of the study area. These shallow depths to the top of magnetic sources are consistent with the relatively thin sedimentary cover of the Sokoto Basin, which locally reaches a maximum thickness of about 300 m before resting unconformably on the crystalline basement. The deeper values (0.34-0.37 km) were concentrated toward the southern region. Depth to centroid (Z_o) values ranged from approximately 3.8 to 7.4 km, with lower values observed in the south-eastern region and higher values trending from the central to north-western parts of the area.

The Curie point depth map (Figure 6(a)) shows values ranging from 4.39 to 14.69 km, with an average depth of 9.13 km. This indicates significant lateral variation in the crustal thermal structure of the study area (Table 1). Shallow Curie depths (4-11 km) were concentrated in the southeastern part of the study area around Maru and Bungudu. These shallow Curie depths are consistent with areas affected by Pan-African granitoid intrusions and Younger Granite complexes (Figure 1), which are known to elevate crustal temperatures through both magmatic heat input and radiogenic decay. The deeper Curie depths

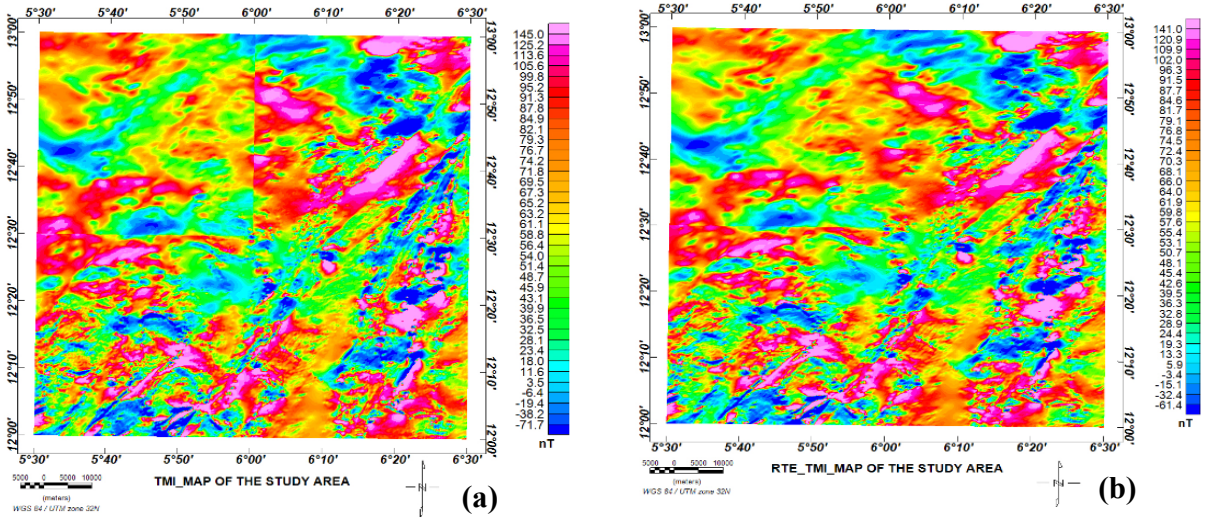

FIGURE 3. (a) Total magnetic intensity of the study area and (b) Reduced to the equator maps of the study area. Both are colour filled contours and histogram equalised. The magnetic 'highs' are shown in red colours and magnetic 'lows' in blue colours

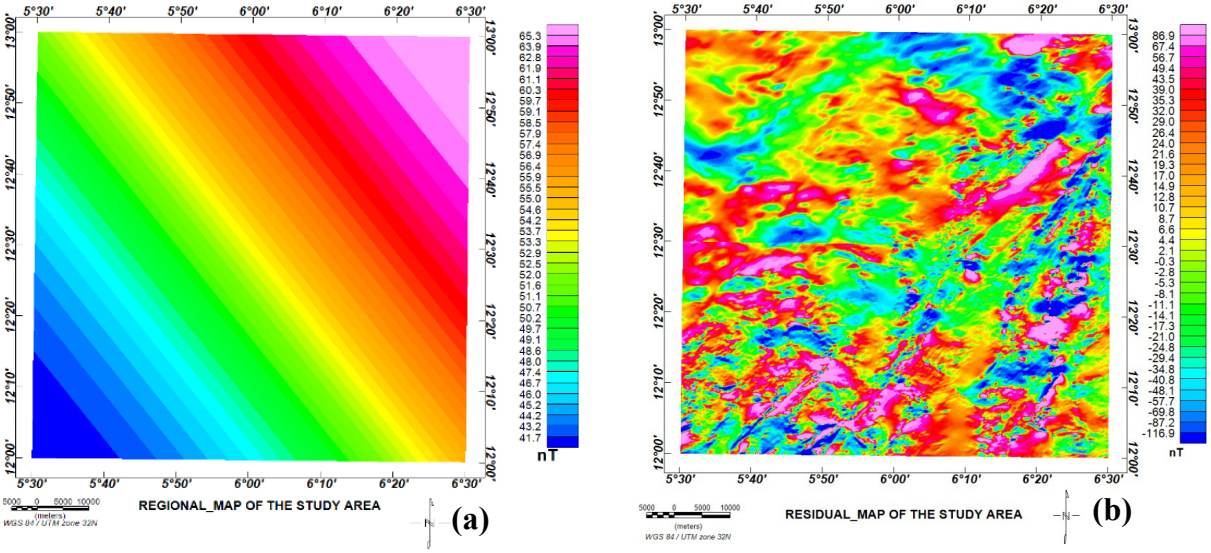

FIGURE 4. (a) Regional magnetic intensity maps of the study area and (b) Residual magnetic intensity maps of the study area showing the effect of removing long wavelength regional from the TMI to produce the residual anomaly map

(12-15 km) occurred mainly in the central region and extended toward the north-western areas, including Kware, Dange Shuni, Tureta, Talata Mafara, and Isa. These variations are consistent with previous studies indicating that Curie depth is strongly controlled by geological and thermal conditions (Nwankwo & Shehu 2015; Tanaka, Okubo & Matsubayashi 1999; Turner 2025). Areas of shallow Curie depth also coincided with zones dominated by sand, clay and medium- to coarse-grained biotite-rich lithologies on the geological map.

The geothermal gradient map (Figure 6(b)), derived from Curie point depths, showed values ranging from 39.47 to 131.89 °C/km, with a mean of 71.26 °C/km as summarised in Table 1. The highest geothermal gradients were observed around Maru and Bungudu, corresponding to areas of shallow Curie depths. On the other hand, lower gradients (35-75 °C/km) were concentrated in the south-western, northern and central regions, including Talata Mafara, Bakura, Anka, and Maradun. Moderate gradients (75-95 °C/km) were observed in the north-eastern, north-western and south-western parts.

The heat-flow map is presented in Figure 7(a). The result showed values ranging from 98.68 to 329.73 mWm^{-2}, with an average of 178.16 mWm^{-2} (Table 1). Extremely

TABLE 1. Summary of spectral depth parameters and derived geothermal properties across the study area, including depth to the top of magnetic sources (Zt), depth to centroid (Zo), Curie point depth (Zb), geothermal gradient (dT/dZ), heat flow (Q), and radiogenic heat production (A)

Blocks	Coordinates		Z_t (km)	Z_o (km)	Z_b (km)	dT/dz (^{0}C/km)	Q (mWm^{-2})	A (μWm^{-3})
1	5.75	12.25	0.34	4.27	8.21	70.65	176.62	3.41
2	5.86	12.25	0.34	3.45	6.56	88.39	220.97	2.89
3	6.00	12.25	0.35	5.54	10.72	54.09	135.22	4.38
4	6.13	12.25	0.32	2.36	4.40	131.89	329.73	2.33
5	6.25	12.25	0.35	4.94	9.54	60.83	152.07	3.89
6	5.75	12.36	0.32	5.31	10.29	56.35	140.87	4.20
7	5.86	12.36	0.33	5.58	10.83	53.58	133.95	4.43
8	6.00	12.36	0.34	5.14	9.93	58.39	145.98	4.05
9	6.13	12.36	0.32	2.44	4.56	127.32	318.29	2.37
10	6.25	12.36	0.36	3.15	5.93	97.79	244.47	2.71
11	5.75	12.44	0.33	5.79	11.25	51.55	128.88	4.62
12	5.86	12.44	0.33	5.63	10.94	53.04	132.59	4.48
13	6.00	12.44	0.34	7.52	14.69	39.47	98.68	6.52
14	6.13	12.44	0.32	2.51	4.69	123.73	309.33	2.40
15	6.25	12.44	0.36	3.45	6.54	88.67	221.66	2.89
16	5.75	12.50	0.32	5.99	11.65	49.77	124.43	4.81
17	5.86	12.50	0.32	5.71	11.09	52.30	130.74	4.55
18	6.00	12.50	0.34	5.36	10.39	55.84	139.61	4.24
19	6.13	12.50	0.32	3.69	7.07	82.09	205.22	3.04
20	6.25	12.50	0.36	5.71	11.05	52.47	131.19	4.53
21	5.75	12.75	0.25	6.92	13.59	42.69	106.71	5.84
22	5.86	12.75	0.33	3.22	6.11	94.92	237.31	2.76
23	6.00	12.75	0.30	4.33	8.35	69.46	173.65	3.46
24	6.13	12.75	0.30	6.51	12.71	45.62	114.04	5.35
25	6.25	12.75	0.32	3.75	7.19	80.72	201.81	3.08
Average			**0.33**	**4.73**	**9.13**	**71.26**	**178.16**	**3.89**

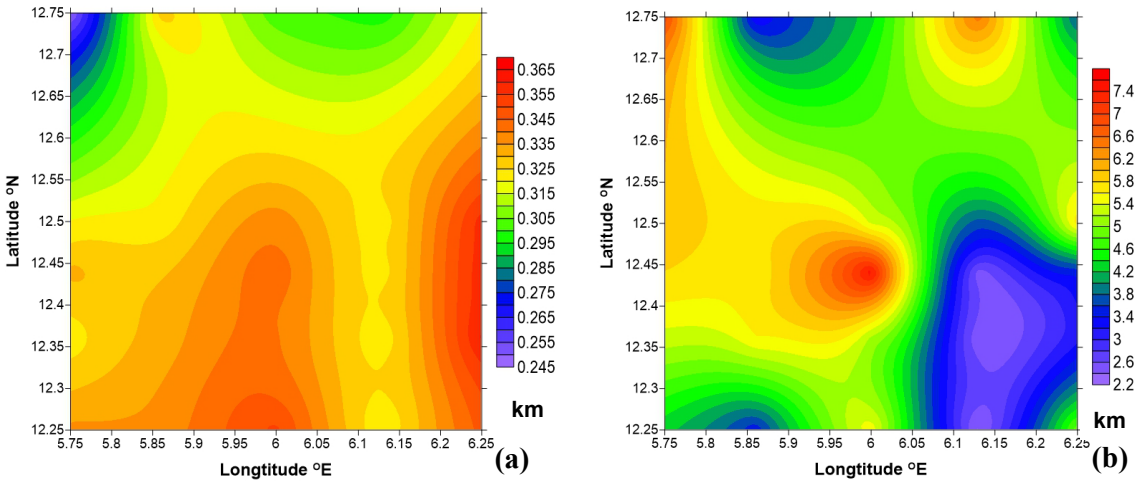

FIGURE 5. Depths to the (a) top (Z_t) & (b) centroid (Z_o) contour maps of the study area showing regions with anomalous depths

high and anomalous heat-flow values (270-330 mWm^{-2}) were recorded in the south-eastern part of the study area around Maru and Bungudu. Moderately high values (90-250 mWm^{-2}) were observed across Talata Mafara, the south-western region, and northern parts of the area. According to established geothermal classifications, heat-flow values exceeding 100 mWm^{-2} indicate anomalous geothermal conditions (Freienstein et al. 2024; Usman et al. 2024). The predominance of such values across the study area suggests favourable geothermal potential. These high heat-flow zones also coincided with basement rocks known to be radioactive in nature.

Radiogenic heat production values vary from 2.32 to 6.51 $\mu W\ m^{-3}$, with an average of 3.89 $\mu W\ m^{-3}$, as presented in Table 1. The radiogenic heat production (RHP) map (Figure 7(b)) further supported the geothermal interpretation. High radiogenic heat production (5.4-6.6 $\mu W\ m^{-3}$) trended from the north-western boundary through the central region to the north-eastern part of the study area. This corresponds spatially to areas dominated by granitic lithologies and migmatite-gneiss units, as shown in the geological map (Figure 1). These elevated values were attributed to granitic and basement rocks enriched in uranium, thorium and potassium, which are known to generate significant radiogenic heat (Salem et al. 2005). Lower RHP values (2.2-5.0 $\mu W\ m^{-3}$) occurred mainly in the south-eastern to north-eastern parts of the study area. Compared with average continental crust values of 2.5-2.9 $\mu W\ m^{-3}$ (McCay et al. 2014), the RHP values obtained in this study are significantly elevated, indicating an anomalous crustal thermal regime that warrants further geothermal investigation.

The geothermal parameters obtained in this study are consistent with, and in some cases exceed, values reported for other regions in Nigeria. Curie point depths ranging between 4 and 15 km are comparable to those reported for the Bida Basin and parts of the Nupe and Anambra basins, where shallow Curie depths were associated with elevated geothermal gradients and heat-flow values (Nwankwo & Shehu 2015). The mean heat flow value of 178 mWm^{-2} obtained in this study is significantly higher than the average continental heat flow of ~65 mWm^{-2} and exceeds values reported for central Nigeria, suggesting a more anomalous thermal regime. Similarly, radiogenic heat production values of up to 6.5 $\mu W\ m^{-3}$ are higher than typical continental crustal averages (2.5-2.9 $\mu W\ m^{-3}$), indicating substantial contribution from radioactive basement rocks. These results collectively suggest that the study area represents one of the more thermally prospective regions within the Nigerian Basement Complex and warrants further geothermal exploration.

INTERPRETATION OF GEOTHERMAL ANOMALIES AND LITHOLOGICAL CONTROLS

The geothermal framework of the study area is defined by a striking degree of heterogeneity. As summarized in Table 1, calculated heat flow (Q) values fluctuate from a relatively stable baseline of 98.68 mWm^{-2} in Block 13 to a localized, intense peak of 329.73 mWm^{-2} in Block 4. While an upper limit of this magnitude is admittedly high for a Precambrian terrain, the spatial convergence of magnetic, radiogenic, and structural information suggests these are not mere mathematical errors, but rather a reflection of a high-energy geological system.

Radiogenic and Lithological Drivers

The primary engine driving this elevated heat flux appears to be a localized enrichment of heat-producing elements. According to the radiogenic heat production (A) data in Table 1, the study area maintains a robust average of 3.89 $\mu W\ m^{-3}$, with specific sectors reaching as high as 6.52 $\mu W\ m^{-3}$. Although the regional model utilized a conservative surface baseline (A_o) of 1.5 $\mu W\ m^{-3}$, the resulting derived values in this study highlight significant *in-situ* contributions from the medium to coarse-grained biotite granites mapped in the sector. These Pan-African 'Older Granites' function as High Heat Production (HHP) units; their radiogenic decay provides the internal thermal energy necessary to shallow the Curie Isothermal Depth (Z_b) to between 4.40 km and 4.69 km in the most active blocks (Blocks 4, 9, and 14).

Structural Control and Thermal Chimneys

The spatial distribution of these thermal hotspots is far from random. The TMI mapping shows that these anomalies align along a distinct N-S to NE–SW trend concentrated around 6.13°E. This trend is clearly evidenced by the longitudinal alignment of Blocks 4, 9, and 14 (Table 1), which consistently exhibit the shallowest Curie depths and highest thermal gradients in the study area. The trajectory that mirrors major regional lineaments of the Anka Schist Belt. Within these high-strain zones, the presence of amphibole schists and highly foliated migmatite-gneisses likely facilitates the formation of 'thermal chimneys'. These deep-seated fractures serve as high-permeability pathways, allowing deep-crustal heat to advect rapidly toward the surface. Conversely, the Sokoto Basin sedimentary cover in the northwest remains a thin skin, with an average depth to the top of magnetic sources (Z_t) of only 0.33 km. This negligible thickness confirms that the sedimentary cover is magnetically transparent and exerts no real influence on deep-seated crustal estimates, which are instead dominated by the underlying basement architecture.

Mathematical Sensitivity and Uncertainty

Finally, the mathematical sensitivity inherent in the spectral analysis is addressed considering the fact that the heat flow equation ($Q = k.\ dT/dZ$) is inversely proportional to the Curie depth (Z_b). The gradient (dT/dZ) becomes exponentially steeper as Z_b shallows toward the 4.4 km limit, reaching a localized peak of 131.89 °C/km in Block 4. To ensure these results were not merely artifacts

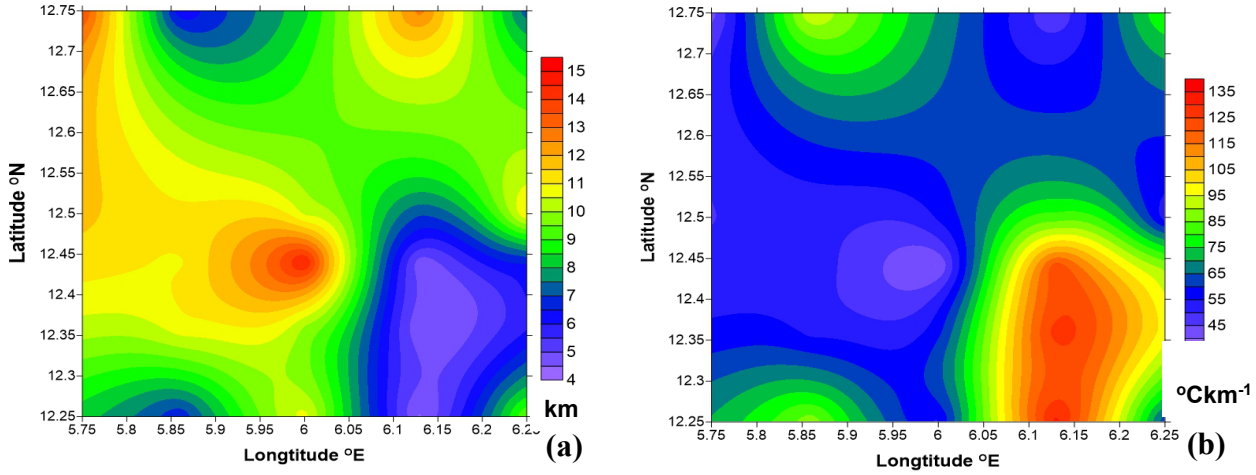

FIGURE 6. (a) Curie point depth (Z_b) & Geothermal gradients (dT/dz) contour maps of the study area showing anomalous regions

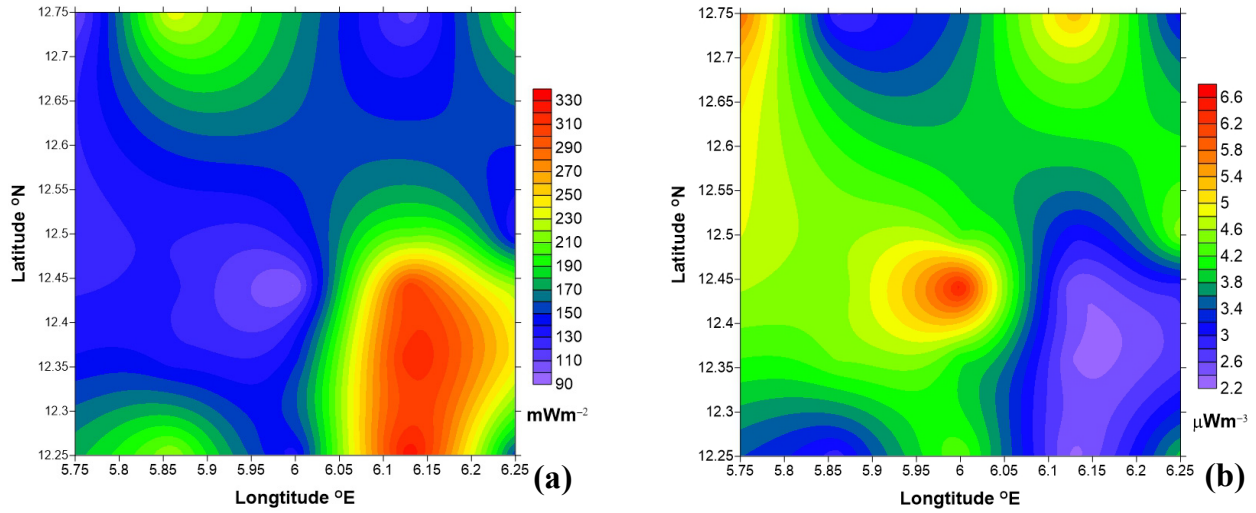

FIGURE 7. (a) Heat flow and b) Radiogenic heat production maps of the study area

of spectral noise, a sensitivity tests was performed by varying window overlaps, which confirmed the stability of these shallow depth estimates. Consequently, the peak values were interpreted as not a regional baseline, but as localized upper-bound thermal anomalies that reflect the complex, heterogeneous thermal evolution of the Zamfara Basement Complex.

Given that the Zamfara region is part of the north-western Nigerian Basement Complex characterized by schist belts, fault-controlled mineralization, and extensive fracture systems, future geothermal investigations should specifically target structurally controlled zones that may act as conduits for heat and fluid circulation. In this context, future studies employing higher-resolution ground magnetic surveys could improve the detection of shallow thermal anomalies. The integration of magnetotelluric (MT) methods for imaging deep conductive fracture zones, high-resolution seismic techniques for mapping fault architecture, and electrical resistivity tomography (ERT) for delineating shallow fractured and weathered zones is recommended. Additionally, detailed structural mapping and geochemical analyses of groundwater and mineralized zones can help identify fluid pathways and heat sources associated with Pan-African tectonic reactivation. Such integrated, structure-focused approaches have been demonstrated to significantly enhance geothermal resource characterization in crystalline basement terrains.

CONCLUSIONS

The aeromagnetic study for geothermal investigation of Northern Nigerian Basement Complex has provided

a detailed understanding of the subsurface geology and thermal structure of the study area. Magnetic data show that the Migmatite-Gneiss Complex, Pan-African Older Granites and Younger Granite ring complexes exert strong control over local magnetic anomalies, with high-intensity regions correlating with granitic intrusions and banded iron formations, while low-intensity areas correspond to thin sedimentary cover of the Sokoto Basin. Spectral depth analysis indicates shallow magnetic sources ($Z_t \approx$ 0.25-0.36 km) associated with near-surface intrusions and deeper sources ($Z_o \approx$ 2.36–7.52 km) corresponding to the Precambrian basement, reflecting the complex basement morphology.

Curie point depth estimates vary between 4.39 and 14.69 km, with shallower depths. This coincides with granitic intrusions and areas of elevated radiogenic heat production, confirming the influence of lithology on the crustal thermal regime. Geothermal gradients range from 39.47 to 131.89 °C/km and heat flow values vary from 98.68 to 329.73 mWm^{-2}, with the highest values concentrated in the Maru-Bungudu region These have suggested significant anomalous geothermal potential. Radiogenic heat production further supports the influence of granitic and migmatitic lithologies, with values reaching up to 6.51 $\mu W/m^3$. These are significantly higher than average continental crust values.

Overall, the study demonstrates that the spatial distribution of magnetic anomalies, Curie point depths, geothermal gradients and radiogenic heat production are strongly controlled by the geological framework, particularly the distribution of granitic intrusions, migmatite-gneiss units and banded iron formations. The results indicate that the study area hosts substantial geothermal potential, especially in regions dominated by heat-producing granitic lithologies. These findings provide a robust basis for future geothermal exploration at the anomalous regions.

ACKNOWLEDGEMENTS

We would like to acknowledge the contributions of the Ministry of Higher Education Malaysia (Fundamental Research Grant Scheme with Project Code: FRGS/1/2022/STG08/USM/03/1 entitled performance – Based Multimodal Geophysical Design for Soil Dynamic Properties to improve Visualization of Subsurface Conditions) and Usmanu Danfodiyo University, Sokoto – Nigeria for their support of this research work.

REFERENCES

Adetona, A.A., Rafiu, A.A., Aliyu, B.S., John, M.K. & Kwaghhua, I.F. 2024. Estimating the heat flow, geothermal gradient and radiogenic heat within the young granites of Jos Plateau North Central Nigeria. *Journal of the Earth and Space Physics* 49(4): 69-81. http://doi.org/10.22059/jesphys.2024.361557.1007538

Aliyu, B. 2024. Geology and geochemistry of Aberma and its environ sheet 54se Gusau, Zamfara State, Nigeria. *Earth Sciences* 13(3): 86-96. https://doi.org/10.11648/j.earth.20241303.11

Boumehdi, M., Hahou, Y., Amrouch, K., Berkat, N.E., Carneiro, J., Correia, A. & Sadki, O. 2025. New assessment of geothermal resources in Morocco: Evaluation of the Curie-point depth method using magnetic data for geothermal gradient and heat flow estimation. *Scientific African* 28*:* e02726. https://doi.org/10.1016/j.sciaf.2025.e02726

Dobrin, M.B. 1976. *Introduction to Geophysical Prospecting.* 3rd ed. New York: McGraw - Hill Book Company.

Ejike, K.N., Egwuonwu, G.N., Obinwa, O., Onyekwelu, C.C. & Ezenwa, N.G. 2025. Assessment of geothermal resource potentials in parts of Central Benue Trough, Nigeria, using aeromagnetic and radiometric data. *Applied Journal of Physical Science* 6(3): 73-90. https://doi.org/10.31248/AJPS2025.116

Freienstein, J., Szwillus, W., Wansing, A. & Ebbing, J. 2024. Statistical appraisal of geothermal heat flow observations in the Arctic. *Solid Earth* 15(4): 513-526. https://doi.org/10.5194/se-15-513-2024

Harash, F. & Chen, C. 2022. Determination of Curie point depth distribution and heat flow regime. *Energies* 15(22): 8634. https://doi.org/10.3390/en15228634

Jiang, X., Zhu, C., Luo, L., Sun, S., Li, D., Fan, K. & Xie, F. 2025. Radiogenic heat production and its contribution to terrestrial heat flow in the eastern Ordos Basin. *Journal of Radio-analytical and Nuclear Chemistry* 334(6): 4041-4052. https://doi.org/10.1007/s10967-025-10153-8

McCay, A.T., Harley, T.L., Younger, P.L., Sanderson, D.C.W. & Cresswell, A.J. 2014. Gamma-ray spectrometry in geothermal exploration: State of the art techniques. *Energies* 7: 4757-4780. https://doi.org/10.3390/en7084757

Muhammad, S.B., Ogunsina, S.A. & Muztaza, N.M. 2025. Geophysical prospecting of mineral potential zones in Zamfara and Environs, Northern Nigeria Basement complex. *UMYU Scientifica* 4(2): 115-121. https://doi.org/10.56919/usci.2542.014

Muhammad, S.B., Muztaza, N.M., Saidu, A., Abdulkadir, M., Abubakar, S. & Mohammed, M.A. 2025. Multi-step filtering of high-resolusion aeromagnetic data over Sokoto Basin, Northern Nigeria. *UMYU Scientifica* 4(2): 109-114. https://doi.org/10.56919/usci.2542.013

Muhammad, S.B., Saad, R., Saidin, M., Muztaza, N.M., Yusoh, R., Sanusi, Y.A., Samuel, Y.M. & Mohammed, M.A. 2020a. Subsurface soil characterisation at Guar Kepah, Kedah Tua (Malaysia) using electrical resistivity tomography for archaeological purpose. *Maejo International Journal of Science and Technology* 14(2): 119-129. http://doi.org/10.13140/RG.2.2.12644.40320

Muhammad, S.B., Saad, R., Saidin, M., Mohammed, M.A., Yusoh, R., Sanusi, Y.A., Samuel, Y.M. & Abubakar, S. 2020b. Analyses of ground magnetic data at Sungai Batu, Kedah, Malaysia in search for buried archaeological remains. *Journal of Physical Science* 31(2): 33-43. https://doi.org/10.21315/jps2020.31.2.3

Muhammad, S.B. & Saad, R. 2018a. Regional structural architecture of part of northern Nigeria basement complex inferred from upward continuation of magnetic field intensity data. *Journal of Physics: Conference Series* 1083: 012057. http://doi.org/10.1088/1742-6596/1083/1/012057

Muhammad, S.B. & Saad, R. 2018b. Hierarchical multiple linear regression for fast estimation of true subsurface resistivity from apparent resistivity measurements based on dipole-dipole array. *Journal of Physics: Conference Series* 1083: 012056. http://doi.org/10.1088/1742-6596/1083/1/012056

Musa, H., Garba, M.A. & Kamureyina, E. 2025. Radially average power spectrum and Curie isotherm from high-resolution aeromagnetic data over Upper Benue Trough, Northeastern Nigeria. *Journal of Engineering Advancements* 6(3): 121-130. https://doi.org/10.38032/jea.2025.03.007

Nwankwo, L.I. & Shehu, A.T. 2015. Evaluation of Curie-point depths, geothermal gradients and near-surface heat flow from high-resolution aeromagnetic (HRAM) data of the entire Sokoto Basin, Nigeria. *Journal of Volcanology and Geothermal Research* 305: 45-55. https://doi.org/10.1016/j.jvolgeores.2015.09.017

Oluyide, P.O., Nwajide, C.S., Oni, A.O. & Rahaman, M.A. 2023. The Nigerian precambrian basement complex: Lithology, tectonics and regional framework. *Journal of African Earth Sciences* 197: 105195. https://doi.org/10.1016/j.jafrearsci.2023.105195

Salem, A., Elsirafy, A., Aref, A., Ismail, A., Ehara, S. & Ushijima, K. 2005. Mapping radioactive heat production from airborne spectral gamma-ray data of Gebel Duwi area, Egypt. *Proceedings World Geothermal Congress* 24–29.

Shlof, A.M.H., Arifin, M.H., Zakaria, M.T. & Salufu, E.O. 2025. Exploration of geothermal resources in Peninsular Malaysia: A review of geological, geochemical, and geophysical techniques. *Journal of Mining and Environment* 16(2): 405-438.

Shuaibu A. M., Abubakar. I. Y. & Garba, M. 2022. Geoelectrical Assessment of Groundwater Potential within Zamfara and its Environs, Northwestern Nigeria. *Caliphate Journal of Science & Technology (CaJoST)* 1: 54-70.

Simon, N., Zulfikri, L.F., Mansor, M.I., Ahmad, Z. & Shahabudin, A.H.S. 2026. Pemetaan gua dan pembangunan parameter saintifik bagi penilaian gua batu kapur sebagai tapak geowarisan: Kajian kes di Gua Bilah dan Gua Persit, Merapoh, Pahang. *Sains Malaysiana* 52(2): 191-208. http://doi.org/10.17576/jsm-2026-5502-02

Sui, D., Wiktorski, E., Roksland, M. & Basmoen, T.A. 2019. Review and investigation on geothermal energy extraction from abandoned petroleum wells. *Journal of Petroleum Exploration and Production Technology* 9: 1135-1147. https://doi.org/10.1007/s13202-018-0535-3

Tanaka, A.Y., Okubo, Y. & Matsubayashi, O. 1999. Curie point depth based on spectrum analysis of the magnetic anomaly data in East and Southeast Asia. *Tectonophysics* 396: 461-470. https://doi.org/10.1016/S0040-1951(99)00072-4

Turner, D.C. 2025. Schist belts of the Benin-Nigeria shield reveal a neoproterozoic supracrustal sequence: Implications for metamorphism and structural evolution. *Precambrian Research* 417: 108500. https://doi.org/10.1016/j.precamres.2024.108500

Usman, M., Abraham, M.E., Okonkwo, C. & Ngene, B. 2024. Thermal energy assessment and structural modelling of the Akiri Hot Spring region, Middle Benue Trough, Nigeria, using magnetic data sets. *Geothermal Energy* 12: 1287. https://doi.org/10.1186/s40517-025-00366-1

Vihywuseh, D., Tabod, C.T., Ndikum, E.N., Khan, A.R. & Fuen, D.A.M. 2025. Unveiling the subsurface geological structure of the Centre Region, Cameroon, with aeromagnetic data analysis. *Scientific Reports* 15: 33296. https://doi.org/10.1038/s41598-025-08077-0

Yusuf, A., Lim, H.S. & Abir, I.A. 2022. Curie-point depths, geothermal gradients and subsurface heat flow estimation from spectral analysis of high-resolution aeromagnetic data. *Sains Malaysiana* 51(3): 657-677. https://doi.org/10.17576/jsm-2022-5103-05

Zakaria, M.T., Muztaza, N.M., Abir, I.A., Ismail, N.A. & Masnan, S.S.K. 2025. Integration of geophysical applications in heterogeneous near-subsurface environments for archaeological investigations. *Sains Malaysiana* 54(2): 343-360. https://doi.org/10.17576/jsm-2025-5402-03

Zakaria, M.T., Ismail, N.A., Muztaza, N.M. & Zaki, M.F.M. 2024. Integrated geophysical models for interpretations of heterogeneous subsurface environments. *Sains Malaysiana* 53(5): 1021-1031. https://doi.org/10.17576/jsm-2024-5305-04

*Corresponding author; email: mmnordiana@usm.my